DOI 10.1007/s10812-022-01311-x
Journal of Applied Spectroscopy, Vol. 88, No. 6, January, 2022 (Russian Original Vol. 88, No. 6, November–December, 2021)

In vitro AND *In silico* ASSESSMENT OF HUMAN SERUM ALBUMIN INTERACTIONS WITH OMEGA 3-6-9 FATTY ACIDS

F. M. Valojerdi,[a] A. Farasat,[b,*] and N. Gheibi[b,*]

UDC 547.962.3

The interaction between human serum albumin (HSA) and omega 3-6-9 fatty acids (omega-3, omega-6, and omega-9), as unsaturated fatty acids, has been investigated using various methods including UV-vis spectrophotometry, circular dichroism (CD) spectroscopy, ELISA, lifetime and fluorescence anisotropy measurements, and the visual molecular dynamics (MD) simulation. The thermodynamic parameters of HSA thermal and chemical denaturation were assessed with and without omega 3-6-9 fatty acids. The T_m and $\Delta G^0_{(298K)}$ of sole HSA were 327.7 K and 88 kJ/mol respectively. These figures for HSA treatment with 10 μM omega-3, omega-6, and omega-9 were 326.2 K and 87 kJ/mol, 319.07 K and 87 kJ/mol, and 313.23 K and 86 kJ/mol, respectively. The same manner of reduction in Gibbs free energy, which is a protein stability criterion, was achieved in chemical denaturation by urea in presence of omega 3-6-9 fatty acids. The interaction of omega 3-6-9 fatty acids with HSA was confirmed after comparing it with L-thyroxin through ELISA assay. Although, evaluation of the regular secondary structure of HSA using CD showed a minor change after incubation with omega 3-6-9 fatty acids, its tertiary structure revealed an observable fluctuation. Thus, it seems that the interaction of omega 3-6-9 fatty acids with HSA leads to instability and partial structural changes. Furthermore, the molecular docking results indicated that the binding affinity of omega-3, omega-6, and omega-9 to subdomain IIA of HSA was higher than subdomain IIIA. These results provide valuable insights into the binding mechanism of omega 3-6-9 fatty acids to HSA, which could play an important role in medicinal drug delivery.

Keywords: *human serum albumin, omega 3-6-9 fatty acids, structure, thermodynamic, L-thyroxin.*

Introduction. Serum albumin (66.4 kDa) is a globular protein of human blood plasma [1]. The protein consists of a single peptide chain of 585 amino acids [2]. Serum albumins are the most abundant soluble circulatory proteins in the blood comprising nearly 52–60% of the plasma. They play the pivotal role as a transporter of various fatty acids, amino acids, hemin, bilirubin, and drug molecules to target sites [3]. The protein has a folded three-dimensional structure, which allows it to carry out the transport function more efficiently. It consists of three high similar domains, containing 17 intrachain disulfide bonds. It should be mentioned here that it has a free cysteine residue at position 34 in domain I and one tryptophan residue at position 214 in domain II. It is suggested that the principal regions of HSA binding ligand are located in hydrophobic cavities in subdomains IIA and IIIA, which are designated as sites I and I, respectively [4]. The binding affinity, offered by site I, is mainly through hydrophobic interaction, while site II involves a combination of hydrophobic, hydrogen bonding, and electrostatic interactions [5]. The HSA extraordinary binding ligand properties reflect its multidomain organization and it is also one of the most important structure–function correlations ever reported for monomeric proteins [6]. It is known that the HSA carries almost every small molecule; thus, it could be a potential candidate as a cargo molecule or a vehicle for clinical, biophysical, and industrial purposes [7, 8]. The protein is considered as an important transporter of various unsaturated fatty acids to the target sites such as omega 3-6-9 fatty acids and hormones including L-thyroxin [9, 10]. Polyunsaturated fatty acids (PUFAs) are fatty acids that contain more than one double bond in their backbone structure. This class of fatty acids include many important compounds such as essential fatty acids. Omega-3 fatty acids (also called ω-3 fatty acids or *n*-3 fatty acids) are PUFAs with a double bond (C=C) at the third carbon atom

*To whom correspondence should be addressed.

[a]Department of Biology, Science and Research Branch, Islamic Azad University, Tehran, Iran; [b]Cellular and Molecular Research Center, Research Institute for Prevention of Non-Communicable Diseases, Qazvin University of Medical Sciences, Qazvin, Iran; email: a.farasat@qums.ac.ir, ngheibi@qums.ac.ir. Abstract of article is published in Zhurnal Prikladnoi Spektroskopii, Vol. 88, No. 6, p. 977, November–December, 2021.

from the end of the carbon chain [11, 12]. Omega-6 fatty acids (also referred to as ω-6 fatty acids or *n*-6 fatty acids) are a family of unsaturated fatty acids which have a common carbon–carbon double bond in the *n*-6 position, which is the sixth bond counting from the methyl end. Linoleic acid or LA (18:2, *n*-6) is the shortest-chained omega-6 fatty acid and also an essential one [13]. Omega-9 fatty acids (ω-9 fatty acids or *n*-9 fatty acids) are also a family of unsaturated fatty acids which have a final carbon–carbon double bond in the omega-9 position. One of the most important omega-9 fatty acids is oleic acid (18:1, *n*-9), which is the main component of olive oil [14]. As mentioned above, the HSA has the ability to bind to a large variety of ligands and deliver them to the target organs as one of the most important carrier proteins. Several studies have proved that molecular dynamics (MD) simulation method has a great role in ligand–receptor recognition in a variety of biological processes. Still, some aspects of the protein structural changes have not been evaluated experimentally [15–17]. Hence, this study is an attempt to prove the physicochemical effects of omega 3-6-9 fatty acids on HSA stability and the structure. Furthermore, their interactions were assessed from thermodynamic, structure, molecular dynamics (MD), and biological points of view.

Materials and Methods. Omega 3-6-9 fatty acids were purchased from Sigma Chemical Company. The stock solution was prepared in buffer (KH_2PO_4 = 0.925 g, $KHPO_4$ = 0.825 g, 169 mL with double-distilled water, pH 6.8). The HSA was also purchased from Sigma Chemical Company. The HSA solution was prepared 30 min before the experiments. The HSA (40 μM) and omega 3-6-9 fatty acids (10 μM) were used in the experiment. For denaturation process, 6 M Urea was prepared. The L-thyroxin was procured from Merck. Solution concentrations of labeled plus unlabeled hormone 15 μM were prepared with a constant HSA concentration. The omega 3-6-9 fatty acids were applied for the test depending on the concentration level.

HSA chemical denaturation. To evaluate the effects of omega 3-6-9 fatty acids on chemical stability of the protein, the HSA chemical denaturation profiles were recorded by titration of a 40 μM protein solution which was aliquoted from a 6 M stock solution of urea. These experiments were performed in absence and presence of omega 3-6-9 fatty acids (10 μM). The protein conformational changes were obtained at 280 nm wavelength using the spectrophotometric technique.

HSA thermal denaturation. The HSA thermal denaturation was carried out using a Spectro fluorimeter (Cary Eclipse model 100 equipped with a thermostatically controlled cuvette compartment). Variable temperatures (10 to 90^{o}C) were applied, and the emission spectra were recorded in 357 nm with the excitation wavelength of 290 nm. The HSA (40 μM) intrinsic fluorescence was measured by thermal scanning both in the absence and presence of 10 μM omega 3-6-9 fatty acids concentrations.

Internal fluorescence. The HSA intrinsic fluorescence measurement in presence and absence of omega 3-6-9 fatty acids was performed via a Spectro fluorometer (Cary model Eclipse) using a 1-cm quartz cell and a thermostat bath. A 40-μM HSA solution was prepared and titrated with increasing concentration of arachidonic acid (0 to 360 μM) in 50 mM buffer solution (temperature 298 K). An appropriate blank, corresponding to the buffer, was subtracted in order to correct background fluorescence. The excitation wavelength was 290 nm, and the emission spectra was recorded from 300 to 420 nm. The maximum emission intensity was used to calculate the binding constant, binding sites occupation, and thermodynamic parameters [18]. The quenching process is described by the Stern–Volmer equation [19]:

$$F_0/F = 1 + K_{SV}[Q] = 1 + k_q\tau_0[Q] , \quad (1)$$

where F and F_0 are the fluorescence intensity with and without the quencher (omega 3-6-9 fatty acids), K_{SV} is the Stern–Volmer quenching constant, and [Q] is the omega 3-6-9 fatty acids concentration.

Binding constant (K_b), number of binding sites (n). When small molecules bind independently to a set of equivalent sites on a macromolecule, the apparent binding constant (K_b) and binding sites number (n) is obtained as follows [20]:

$$\log (F_0 - F/F) = \log K_b + n \log [Q] , \quad (2)$$

where F_0 and F are the fluorescence intensities before and after the addition of the quencher, respectively, and [Q] is the total quencher concentration.

Thermodynamic parameters and the binding forces. The interaction forces between a drug and biomacromolecule may include hydrophobic forces, electrostatic interactions, van der Waals interactions, hydrogen bonds, etc. To elucidate the energy changes of the ligand–protein interaction, the thermodynamic parameters were calculated using van't Hoff plots. If the enthalpy (ΔH) does not vary significantly over the studied temperature range, then the value and the entropy change (ΔS) can be determined using the van't Hoff equation:

$$\ln K_b = -\Delta H/RT + \Delta S/R\,, \tag{3}$$

where K_b is binding constant at the corresponding temperature and R is the gas constant. The enthalpy change (ΔH) is calculated from the slope of the van't Hoff relationship. The free-energy change (ΔG) is estimated from the following [21]:

$$\Delta G = \Delta H - T\Delta S\,. \tag{4}$$

HSA and omega 3-6-9 fatty acids structural analysis using CD. The CD measurements were carried out using a JASCO spectropolarimeter (model J-800) equipped with a thermoelectrically controlled cell holder under a constant nitrogen flow. Cuvettes with path lengths of 1 mm were applied. Far-UV-CD spectra were recorded in the range of 190–260 nm and near-UV-CD, and the adjacent chain of aromatic amino acids was absorbed in the range of 290–250 nm. An HSA concentration of 40 μM and an omega 3-6-9 fatty acid concentration of 0, 20, 80, and 100 μM were used respectively. The slit width was set at 5 nm, and the scanning speed was 30 nm/min [22].

Evaluation of L-thyroxin and omega 3-6-9 fatty acids binding to HSA via ELISA method. The total T4 ELISA test kit (ACON Biotech Co., China) was used in the enzyme immunoassay for the quantitative detection of total thyroxin concentration in human serum. The experiments were performed at 25°C with media, buffered with 50 mM potassium phosphate (pH 6.8). Different concentrations solutions of labeled plus unlabeled hormone (15 μM) were prepared with a constant HSA concentration (40 μM). The competitive interaction of omega 3-6-9 fatty acids and L-thyroxin with HSA was carried out using ELISA technique at a wavelength of 450 nm. The free and the binding L-thyroxin were assessed (μg/dL) and the concentration (μg/dL) was read from the horizontal axis of the graph [23].

Lifetime measurements (τ_F). The fluorescence lifetime measurements were performed using an Edinburgh Instruments (FLS 920) spectro fluorimeter in laser mode with excitation and emission wavelengths of 255 and 320 nm, respectively. The spectro fluorimeter in photon counting mode equipped with a temperature-controlled cell was connected to a circulating water bath. Fluorescence lifetime of 40 μM HSA in buffer phosphate (pH 7) was measured in the presence and absence of 100 folded omega 3-6-9 fatty acids concentrations. Using a double-exponential decay function of the decay profiles with F900 analysis software, the lifetime values were determined from the deconvolution fit analysis. The goodness of fit was assessed by applying the reduced χ^2 value (close to 1 in all cases).

Furthermore, based on the following equation and using the amplitude β_i of the ith component lifetime τ_{Fi}, the average fluorescence lifetime (τ_F) was calculated since TRP and α-Lac present two different lifetime values [24]

$$\tau_F = \Sigma_i \beta_i \tau_{Fi}^2 / \Sigma_i \alpha_i \tau_{Fi}\,. \tag{5}$$

Fluorescence anisotropy measurements. Fluorescence anisotropy is a phenomenon where the light emitted by a fluorophore has unequal intensities along different axes of polarization. The steady-state anisotropy (r) is given by the following:

$$r = I_{VV} - G\,I_{VH}/I_{VV} + G_2 I_{VH}\,, \tag{6}$$

where I_{VV} and I_{VH} are the intensities measured by vertically polarized excitation, as indicated by the first subscript and detected through vertically and horizontally oriented emission polarizers, respectively, as indicated by the second subscript. The factor $G\,I_{HV}/I_{HH}$, which is measured using horizontally polarized excitation, corrects the instrument polarization bias. Fluorescence spectra and steady-state emission anisotropies of all HSA samples were measured with Cary Eclipse fluorimeter (Agilent, Palo Alto, CA). Anisotropy was measured by a manual polarizer, and the G factor correction was done manually, with a reference fluorophore. The labelled protein was then excited at start point of 635 nm and stop point of 640 nm. Then the parallel and perpendicular emissions were monitored at maximum emission of 580 nm with a manual polarizer. The anisotropy measurement of the protein was then repeated with omega 3-6-9 fatty acids [25].

Protein–ligand docking process. The geometries of omega-3, omega-6, and omega-9 fatty acids were obtained from PubChem, while the crystal structure of HSA (entry code: 4K2C) was downloaded from Protein Data Bank (http://www.rcsb.org). The omega-3, omega-6, and omega-9 fatty acids molecular docking process to HSA was examined through a commutable docking process. The side chain of the receptor and ligand had enough flexibility and were able to interact with HSA chains through Auto Dock Vina [4]. Autodock (version 1.5.6) was applied to define the ligand permissible torsions, append the polar hydrogen atoms to the protein, and characterize the search space coordinates. The IIA and IIIA domains in HSE were capable of forming a bond with the ligand on $X = 26$, $Y = 42$, and $Z = 34$ in 1 Å spacing. Autodock

has the capability to determine the lowest binding energy of omega-3–HSA (domain II), omega-6–HSA (domain II), omega-9–HSA (domain II), omega-3–HSA (domain III), omega-6–HSA (domain III), and omega-9–HSA (domain III) complexes for docking conformation that were assumed as early conformations for MD simulation.

Molecular dynamics analysis of HSA–fatty acids. The conformational modifications of the ligand–enzyme complex were measured using MD method, the GROMOS96 43a1 force field, and the GROMACS 4.5.4 package software [26]. The complexes provided by the aforementioned method were placed into a [simulation] box full of water molecules. Then, the GROMACS measured the HSA topology parameters. Furthermore, the omega 3-6-9 fatty acid topology characteristics were obtained from the Dundee PRODRG server [27]. Next, a box of simple point charge water molecules was provided and the aforementioned complex was immersed in it. To minimize the energy, the steepest descent method for 10,000 steps, followed by the conjugate gradient method for 10,000 steps, was applied for inconsistent contact releases. The equilibration phase of the system (position-restrained dynamics simulation, NVT/NPT) was carried out at 300 K for 200 ps, followed by MD production run for 20 ns [28, 29]. The atomic coordinates were recorded every 2.0 ps within the MD simulation.

Results and Discussion. *Chemical and thermal denaturation.* Chemical and thermal denaturation profiles were obtained from urea titration and thermal scanning with and without omega 3-6-9 fatty acids in definite concentrations (Figs. 1 and 2). Each profile is a sigmoidal curve; thus, this process is described as a single denaturant-dependent step based on the two-step theory. Proteins do the most demanding jobs in living cells. For this reason, they must interact specifically with other molecules. In order to achieve the purpose, the polypeptide chain folds to a unique, globular conformation, which is called the native state of the protein and denoted by N. This is the structure that can be determined in crystals via X-ray crystallography or in solutions using NMR. The native state is only marginally more stable (generally 2–10 kcal/mol under physiological conditions) than the large ensemble of unfolded states that we call the denatured state of the protein and denote by D. The equilibrium between these two macros can be stated as N ↔ D.

The conformational stability of a protein is

$$\Delta G^0 = G_{\mathrm{D}} - G_{\mathrm{N}} = -RT \ln K, \tag{7}$$

where G_{D} and G_{N} are the free energies of D and N, respectively; K and ΔG are the equilibrium constant and standard free energy changes. The determination of standard Gibbs free energy of denaturation (ΔG^0), as a conformational stability criterion of a globular protein, is based on the two-state theory and the second Eq. (7).

The secondary plots of Figs. 1 and 2 are illustrated in insets. From these linear plots, the ΔG^0 varies linearly with denaturant agent (urea concentration and temperature) over a limited region:

$$\Delta G^0 = \Delta G^0_{\mathrm{H_2O}} - \mathrm{m}\left[\mathrm{denaturant}\right],$$

where $\Delta G^0_{\mathrm{H_2O}}$ is the free energy of conformational stability in the absence of denaturant and m is the ΔG^0 dependence measure in denaturant concentration.

In chemical denaturation, the $[\mathrm{UREA}]_{1/2}$ is the denaturant concentration that the protein needs to complete half of its two-state transition. In thermal denaturation, protein melting point (T_{m}) is the temperature which the protein requires to complete half of its two-state transition. The magnitudes of the $\Delta G^0_{\mathrm{H_2O}}$, $[\mathrm{UREA}]_{1/2}$, and T_{m} determined based on plots are summarized in Table 1 [30].

Fluorescence characteristics of HSA quenched by omega 3-6-9 fatty acids and the binding mode mechanism. The HSA is a single-string globular protein with 6500 amino acids, in which the tryptophan 214 residue was used to measure the fatty acids-binding affinity. The HSA intrinsic fluorescence is very sensitive to its microenvironment. When the HSA local environments are altered slightly, its intrinsic fluorescence is weakened. Several factors such as protein conformational modifications, biomolecular binding, and denaturant are responsible for the fluorescence weakening. In our experiments, the pH value was maintained at 6.8 and the temperature was below 298 K and under this condition, HSA was not denaturized. The HSA concentrations were stabilized at 40 μM, and the fatty acid contents varied from 0 to 360 μM. The effects of fatty acids on HSA fluorescence intensity is shown in Fig. 3. The HSA fluorescence intensity decreases along with the increase in omega 3-6-9 fatty acid concentration. A higher excess of fatty acids leads to a more effective chromophore molecule fluorescence quenching, which suggests that fatty acids quench the HSA intrinsic fluorescence [31, 32].

Stern–Volmer analysis. To determine the HSA binding mechanism to omega 3-6-9 fatty acids, the fluorescence intensity data were analyzed by the Stern–Volmer equation. Fluorescence quenching is usually classified as dynamic and

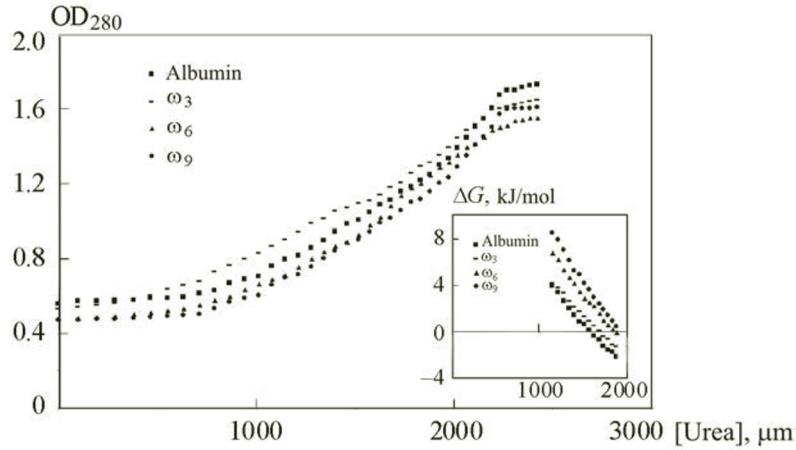

Fig. 1. UV-vis absorbance spectra of chemical denaturation after titration by urea in the concentration of HSA 40 μM and its interaction with omega-3, omega-6, and omega-9. Inset: secondary plot of the two-state chemical denaturation.

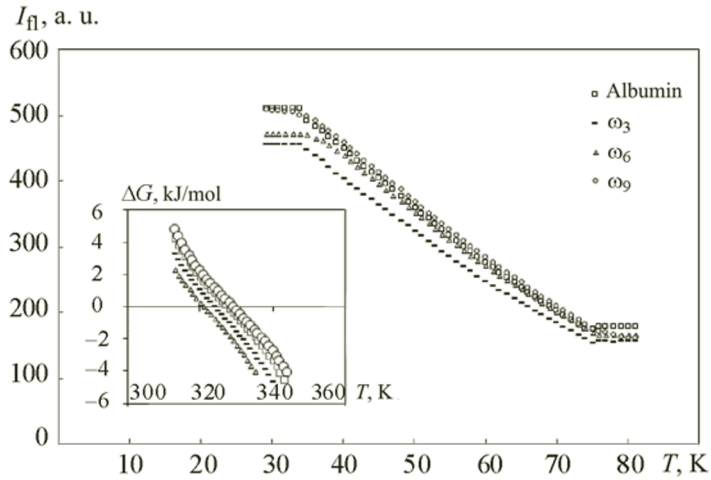

Fig. 2. Thermal denaturation curve obtained from emission internal fluorescence of HSA 40 μM; and its interaction with omega-3, omega-6, and omega-9. Inset: secondary plot of two-state thermal denaturation.

TABLE 1. Thermodynamic Parameters Obtained from Chemical and Thermal Denaturation Curves of HSA/AA Interactions

Sample	Chemical denaturation			Thermal denaturation	
	$[Ligand]_{1/2}$, M	ΔG_{H_2O}, K/mol	M, K/mol	T_m, K	$\Delta G^0_{[298K]}$, K/mol
HSA	0.16	13.19	83	327.70	88
HSA/ω_9	0.15	12.70	82	326.20	87
HSA/ω_6	0.14	10.52	73	319.07	87
HSA/ω_3	0.12	7.46	60	313.23	86

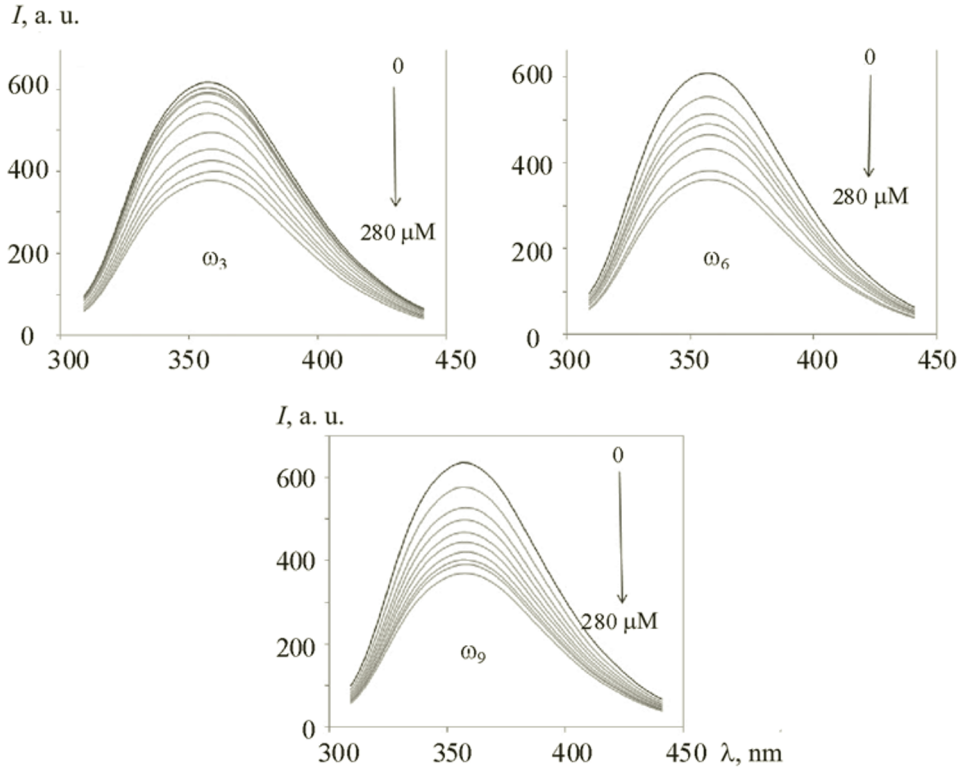

Fig. 3. Effect of omega 3-6-9 fatty acids on fluorescence spectrum of HSA (T = 298 K, λ_{exc} = 290 nm) with the concentration of HSA = 40 μM and AA = 0, 40, 80, 120, 160, 200, 240, 280 μM.

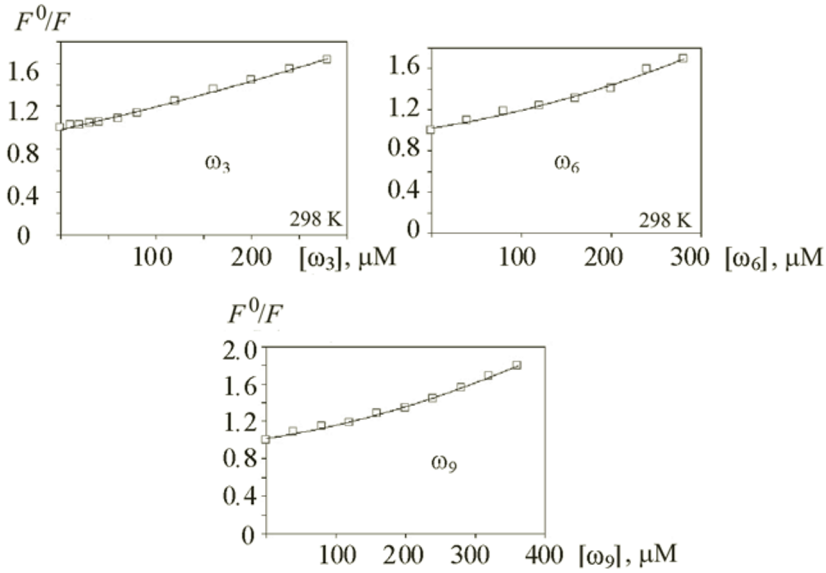

Fig. 4. Stern–Volmer curve for the interaction HSA–omega 3-6-9.

static quenching [33]. However, the Stern–Volmer plot showed a minor positive deviation (Fig. 4), indicating the presence of both static and dynamic quenching. The Stern–Volmer quenching constant was calculated using the equations listed in Table 2.

TABLE 2. Binding and Thermodynamic Parameters Obtained from the Interaction of HSA with ω_3 [6–9]

Sample	T, K	n	R	$10^4 K_{SV}$, L/mol	ΔG^0, kJ/mol	ΔH^0, kJ/mol	ΔS^0, J/mol·K
HSA/ω_9	298	0.8	0.99	4.9	29.52	–13.70	125.80
HSA/ω_6	298	0.7	0.98	6.1	21.15	–12.42	112.60
HSA/ω_3	298	1.2	0.99	5.8	10.12	–17.52	92.75

Secondary structural analysis of HSA and omega 3-6-9 fatty acids. The HSA far-UV-CD spectra exhibited two negative bands at wavelengths 208 and 222 nm, which are the characteristic of β-sheet and α-helical protein structures. The near-UV-CD obtains the HSA third regular structure values. When the omega 3-6-9 fatty acids concentration is increased gradually from 20 to 100 μM, the changes are shown basically thorough CD (Figs. 5 and 6) [34].

Calculation of HSA binding to L-thyroxin with and without omega 3-6-9 fatty acids via ELISA. The magnitudes of L-thyroxin binding to the HSA with and without ω_9, ω_6, and ω_3 fatty acids were equal to 22.28, 20.49, 20.61, and 20.82, respectively.

Lifetime measurements. Based on fluorescence lifetime measurements results, adding 20 and 100 μM of omega 3-6-9 fatty acids to the protein solution caused no significant changes to fluorescence lifetime.

Anisotropy. The HSA was labeled with CD, and the anisotropy of the labeled protein was measured before and after omega 3-6-9 fatty acids binding. The dye–protein ratio was low, and the anisotropy of unlabeled protein was 0.28. When omega 3-6-9 fatty acids was added to the labeled protein, the anisotropy decreased to 0.26. As is shown from the HSA and omega 3-6-9 fatty acid interaction, the third structure are not stable. This could be attributed to HSA conformational changes and generation of another binding site upon interaction with omega 3-6-9 fatty acids, which is in agreement with our CD and anisotropic findings [35].

Molecular docking and molecular dynamics. Molecular docking was performed to evaluate the interaction of the omega-3, omega-6, and omega-9 fatty acids with specific binding sites on HSA. The binding location of the omega-3, omega-6, and omega-9 fatty acids with the HSA molecule is of great importance, because any information about protein–ligand binding interaction can help us understand their function and efficacy as potential therapeutic agents [32]. The AutoDock Vina docking software contains an important option essential to the present study, which is the selective side-chain residue flexibility [33]. The main advantage of this option is to provide a more pragmatic approach to ligand–protein interaction without a notable increase in computer processing time. The conformational modifications that occur within the receptor may impart major concepts and demonstrate that the receptor flexibility is an important part of computational drug design that has been mentioned above [34]. To measure the structural changes that are caused by ligand binding (omega-3, omega-6, and omega-9), MD simulations of free HSA (subdomain II and III) and six complexes of (omega-3/omega-6/omega-9)–HSA (subdomain II and III) were carried out, and the results were compared. In the next step, three parameters including the root mean square deviations (RMSD), root mean square fluctuations (RMSF), and the secondary structure were studied. Based on the obtained results from previous parts, evaluation and comparison of the HSA protein stability was possible during the MD simulation period. The time needed for RMSD progress from the early structure was computed for four simulation runs. The RMSDs of Cα-atoms are displayed in Fig. 7. Based on the results, after 1 ns, the protein involved in the complex and the free protein became stable enough, which represents equilibration in the system. The RMSD values of the HSA Cα-atoms and the complexes that were discussed above demonstrated that all systems obtained enough equilibration and average oscillation. They also kept their stability until the end of the simulation process (Fig. 8). The RMSF was used to obtain flexibility information. The protein Cα atoms RMSFs displayed in Fig. 9a,b indicate the molecular flexible regions. The RMSF value for the free protein and the protein involved in the complex have similar trends as illustrated in Fig. 9, while residues 262–267 and 474–480 in subdomain IIA and IIIA have the highest RMSF values. Due to molecular movement restriction which was induced by the ligand, the free protein demonstrates a higher RMSF value compared to the protein involved in the complex. As illustrated in Fig. 9a,b,c, in site I of HSA, the omega-3/omega-6/omega-9–HSA complexes were formed by hydrophobic interaction. In site II, omega-3–HSA and omega-6–HSA complexes were formed by hydrophobic interaction (Fig. 9b,d). As for omega-9–HSA complex, the interface was established by hydrophobic and H-bond interaction with the following amino acids: Lys402 and Ala406 (Fig. 9e,f). In site I, the affinity of omega-3, omega-6, and omega-9 with HSA was –6,

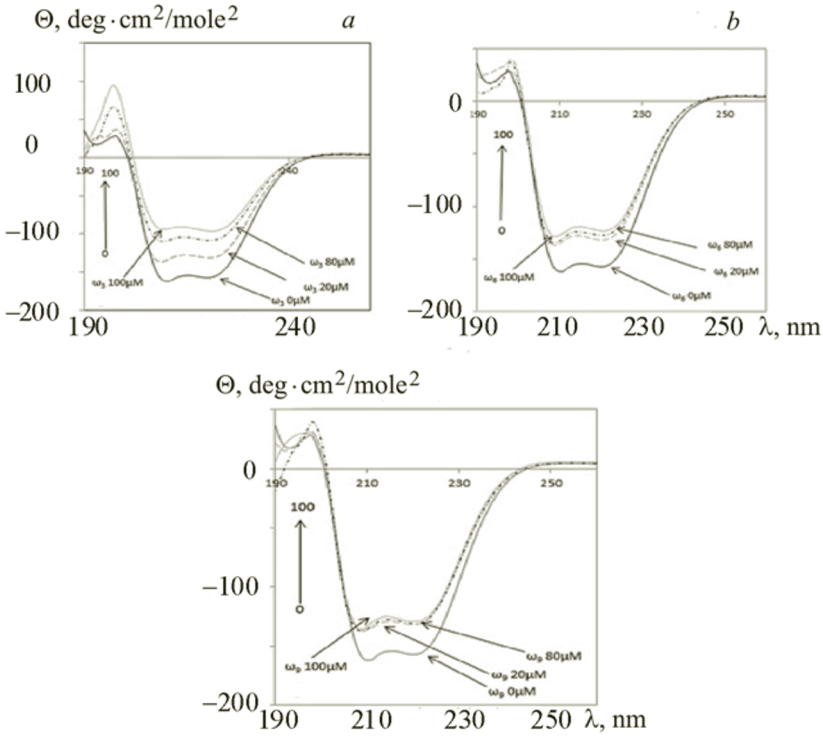

Fig. 5. Far-UV-CD spectra of the HSA–omega3-6-9 fatty acid interaction: HSA = 40 μM and omega-3-6-9 = 0, 20, 80, and 100 μm.

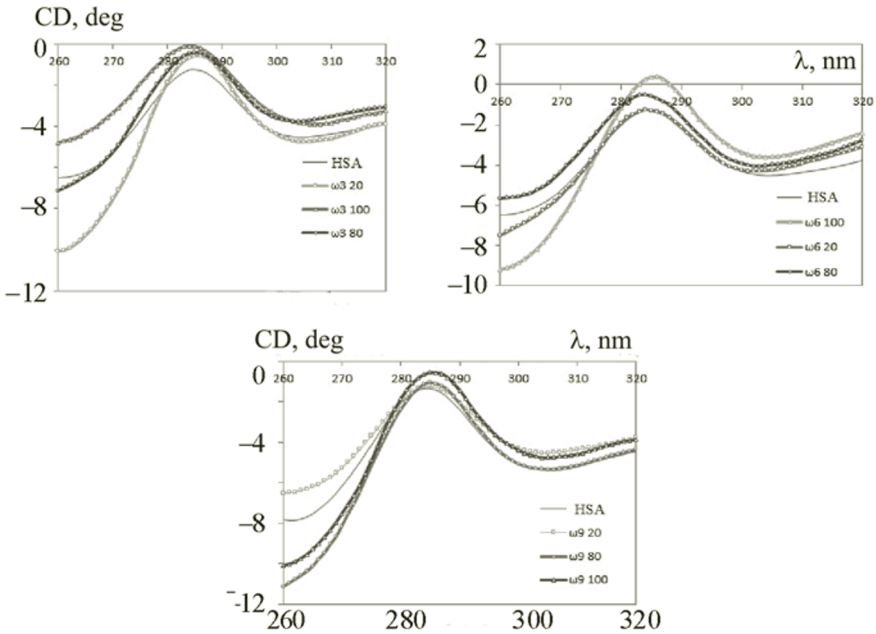

Fig. 6. Near-UV-CD spectra of the HSA–omega3-6-9 fatty acids interaction: HSA = 40 μM and omega-3-6-9 = 0, 20, 80, and 100 μm.

–5.6, and –5.4 kcal/mol, respectively. Furthermore, in site II, the affinity of omega-3, omega-6, and omega-9 with HSA was –4.9, –4.9, and –4.8 kcal/mol, respectively. These results indicate that omega-3, omega-6, and omega-9 bind more effectively to the large hydrophobic cavity of HSA at site I than site II.

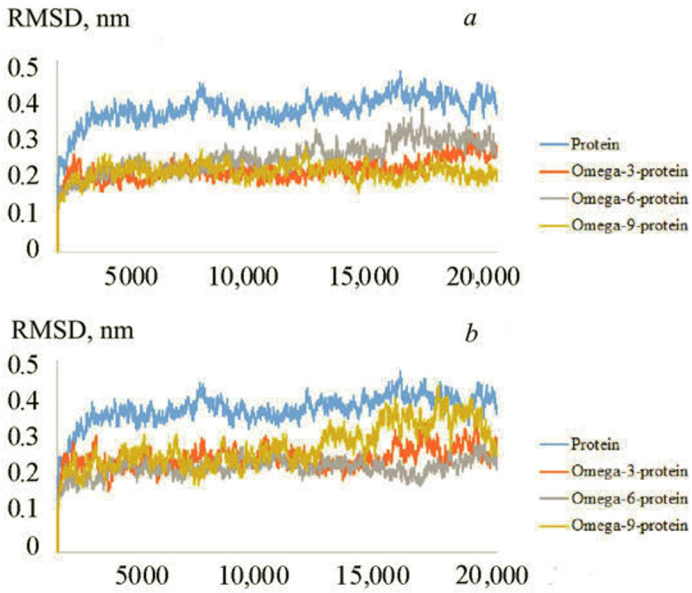

Fig. 7. The RMSD values of carbon-α of free HSA and HSA in complex with omega-3, omega-6, and omega-9 in site I/II (a/b).

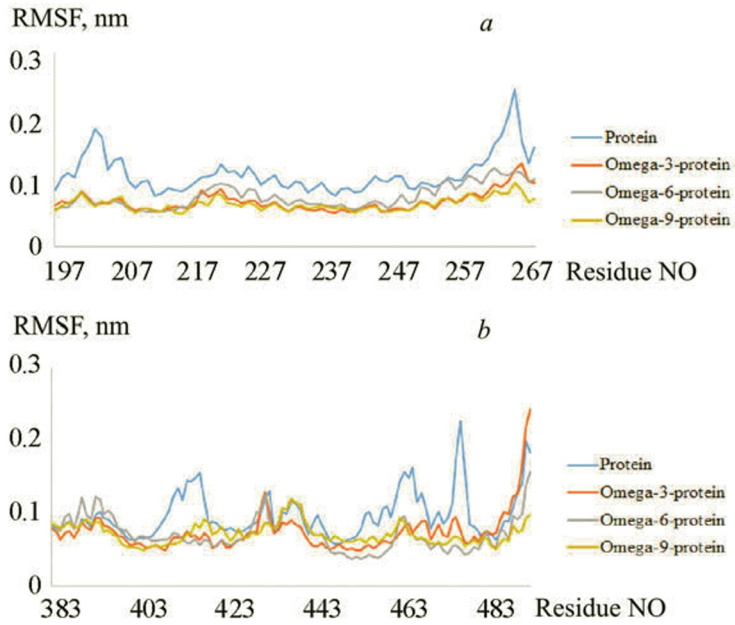

Fig. 8. The RMSF values of free HSA and HSA in complex with omega-3, omega-6, and omega-9 in site I/II (a/b).

Discussion. Albumin is the most abundant plasma protein and serves as a transport and depot protein for numerous endogenous and exogenous compounds [36]. Thermodynamic parameters of chemical and thermal denaturation plots of HSA and omega 3-6-9 fatty acids were examined. The Gibbs free energy and the protein T_m decreased after incubation with omega 3-6-9 fatty acids. This instability was proved by fluorescence structural and CD studies and also by the omega 3-6-9 fatty acids–L-thyroxin functional competition to interact with HSA. The omega 3-6-9 fatty acid binding effects on the unfold HSA equilibrium were investigated by urea-induced denaturation as monitored by spectrophotometric measurements after the protein excitation at 280-nm wavelength.

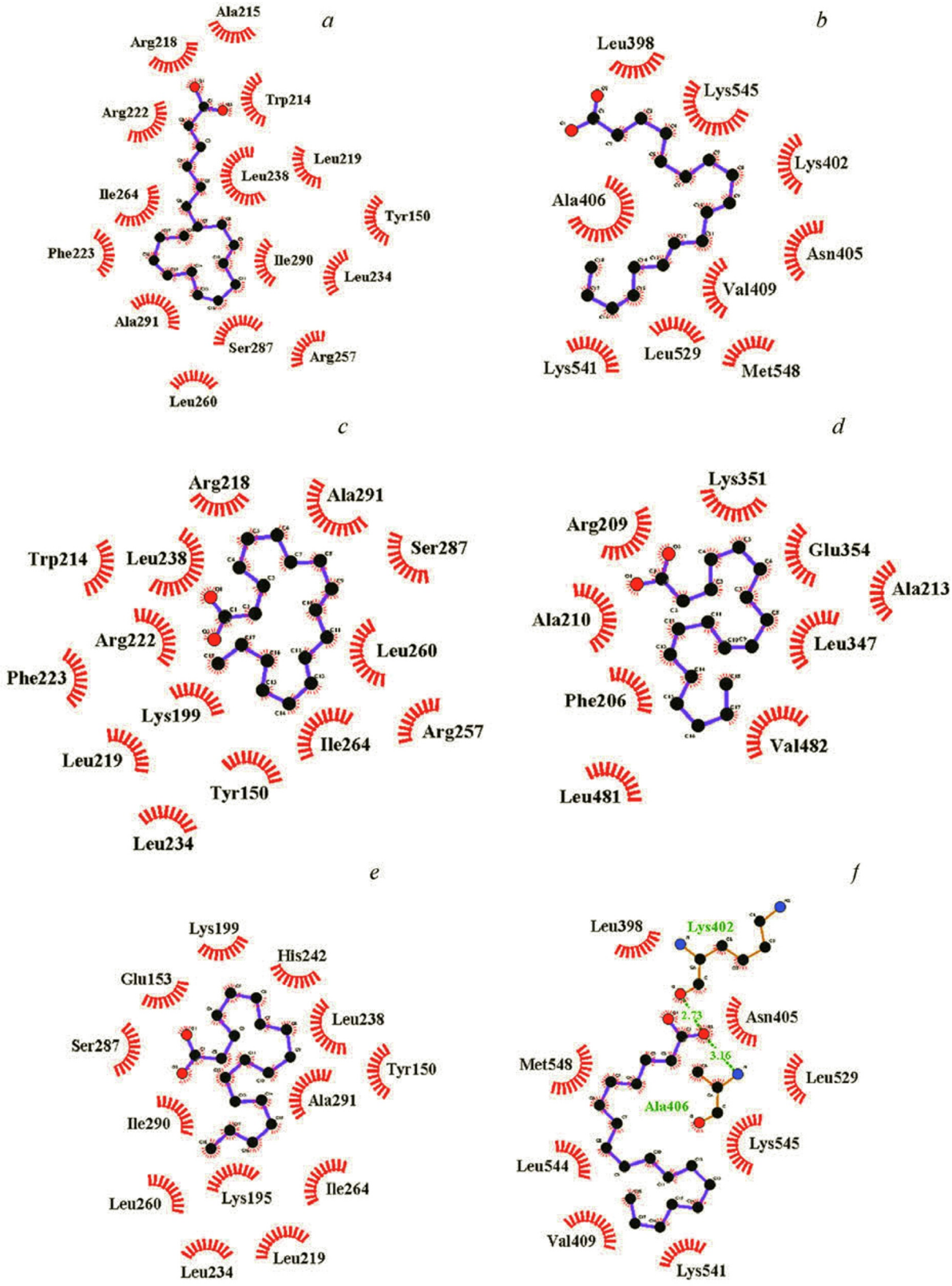

Fig. 9. The best conformations of omega-3–HSA (a,b), omega-6–HSA (c, d), and omega-9–HSA complexes (e, f) in site I (a, c, e) and II (b, d, f).

The stabilization of free energy (ΔG_{H_2O}) in the absence and presence of omega 3-6-9 fatty acids were equal to 13.19, 12.7, 10.52, and 7.46 kJ/mol as determined by linear fittings of intrinsic spectrophotometric data. Our findings indicated that the thermodynamic parameters (C_m and the ΔG_{H_2O} values) that were obtained from denaturation method expressed the same relative protein instability (Table 1). The parameter chosen to compare the transition curve is the melting temperature (T_m), which is defined as the midpoint of the denaturation process and calculated by plotting the first derivative of the values as a function of temperature (Fig. 2). These parameters indicate unstable HSA (Table 1). The results indicated that urea interacts with HSA by electrostatic forces, yielding a randomly coiled conformation in its unfolded state, while thermal denaturation produces a molten globule state and the protein aggregation. Therefore, the both methods yield different structurally unfolded HSA states. In the present study, evaluating the binding parameters of HSA–CF (TP or TB) complex that were calculated from the van't Hoff equation yielded ΔH = 47.72, 15.95, 38.90 kJ/mol, ΔS = 242.03, 136.96, 213.58 kJ/mol, ΔG = –24.73, –25, –24 kJ/mol. Based on efonidipine interaction with BSA, ΔH = 68.04 kJ/mol, ΔS = 319.42 kJ/mol, and ΔG = –27.08 kJ/mol were obtained. Hence the positive ΔH and ΔS values are associated with hydrophobic interactions [37].

Based on the results, the negative value of ΔG^0 obtained from Stern–Volmer data analysis (Table 2) identified that HSA binding to omega 3-6-9 fatty acids is a spontaneous process. The positive ΔH^0 and ΔS^0 values for omega 3-6-9 fatty acids indicate that the forces acting between these compound and omega 3-6-9 fatty acids is mainly a hydrophobic interaction. Thus, the HSA nonpolar hydrophobic groups may be responsible for the main effect of omega 3-6-9 fatty acids –protein binding [38]. As demonstrated in Table 2, the K_{SV} values can be achieved based on the slope. In addition, K_{SV} of omega 3-6-9 fatty acid treatments with HSA suggest that the overall quenching is dominated by dynamic quenching [38]. Nevertheless, the number of binding sites suggests that the binding site for omega 3-6-9 fatty acids on HSA is primarily on Trp-212 residue, which is located within a hydrophobic binding pocket of the protein. The thermodynamic parameters of fluorescence techniques showed HSA instability in presence of the omega 3-6-9 fatty acids.

The HSA CD spectra in the absence and presence of B12 and 4-thio-5-methyluridine exhibited two negative bonds in UV region of 209 and 228 nm of β-sheet and the helical structure of protein. The results showed that B12 and 4-thio-5-methyluridine have fundamental effects on HSA secondary structure. Furthermore, the regular HSA secondary structure obtained by CD showed a minor change after incubation with omega 3-6-9 fatty acids.

The HSA is a transporter for thyroxine and also other hydrophobic compounds, including fatty acids. In this study, we provided structural insights of the factors that mediate the T4 to HSA binding process and the effects of fatty acids on HSA binding. The results demonstrated that the omega 3-6-9 fatty acid binding to HSA decreases the L-thyroxin hormone on the albumin site because the omega 3-6-9 fatty acids are in the HSA positions and can play an inhibitory role for the L-thyroxin hormone.

The main purpose of this study was evaluating the binding properties of HSA and fatty acids due to the great importance of the binding process in pharmacology and biochemistry. The interaction of fatty acids with HSA was studied by spectroscopic methods including fluorescence spectroscopy, UV-vis absorption spectroscopy, and CD techniques. The results demonstrated that the conformation of HSA molecule changed basically in presence of fatty acids. The results also showed that the HSA fluorescence was quenched by fatty acids through static quenching. It could be deduced that the bonding mode in the binding reaction between fatty acids and HSA was mainly due to its hydrophobic nature, which is estimated from ΔH and ΔS. Synchronous fluorescence spectra showed that the tryptophan residue micro-environmental changes are mostly hydrophobic. The HSA secondary and tertiary structural changes in presence of fatty acids were investigated by CD spectroscopy. The results obtained by CD from regular secondary structure of HSA after its interaction with different concentrations of omega 3-6-9 fatty acids (Fig. 5) and near-UV-CD are in agreements with our data achieved by CD from regular HSA tertiary structure with the same conditions (Fig. 6). As mentioned, the HSA is a transporter for thyroxine and other hydrophobic compounds such as fatty acids. To obtain an appropriate structural and functional effect by the interaction of omega 3-6-9 fatty acids with the protein, its competition with T4 was proved after the reduction of T4 binding to HSA. This reflects lifetime measurements in which the interaction between HSA and omega 3-6-9 fatty acids are due to the static nature. Hence, the omega 3-6-9 fatty acids are in dynamic equilibrated interaction with specific sites in HSA [13]. Moreover, this study illustrated the HSA binding nature (domain A).

Several previous studies have shown that subdomains IIA and IIIA could be considered as target sites for docking process, and this phenomenon is due to the fact that they are assumed to be early drug binding sites [35–37]. Evaluating other sites to find an appropriate site for MD simulation could be more beneficial. To study the structural changes caused by the ligands (omega-3, omega-6, and omega-9 fatty acids) binding, we performed MD simulation of HSA and IIA-

IIIA omega-3, omega-6, and omega-9 fatty acids subdomains and consequently compared the obtained results. In the current study, the interaction of omega-3, omega-6, and omega-9 with HSA was investigated using spectroscopic methods and MD. Protein stability in solution is a subject of substantial interest for biologists and pharmacologists. The docking and molecular simulation outcomes revealed that omega-3, omega-6, and omega-9 could efficiently bind to subdomains IIA (site I) of HSA. In conclusion, Various trigger mechanisms are involved in the interaction of omega-3, omega-6, and omega-9 fatty acids with human serum albumin: 1) Diffusion, which is governed by the physicochemical properties of materials and occurs when the wall structure is intact; 2) structural change, which is triggered by the addition of omega-3, omega-6, and omega-9 to binding with HSA; 3) dissolution, which results from the use of solvent to expand materials and favor the release; 4) pH and ionic strength changes, which alter the solubility of materials; and 5) high temperature, which is able to bind or collapse [38].

Conclusions. Based on structural and functional relationship, studying HSA as the most important protein carrier is necessary to examine structural changes with and without ligands. These changes can be explained by the nature of non-covalent physical interactions and the ligand induced minor instability and flexibility. Consequently, our findings showed ω-9 > ω-6 > ω-3 instability patterns in the protein structure.

Acknowledgments. We gratefully acknowledge financial support from the educational department of Azad University of Science and Research, Qazvin University of Medical Science and Biochemistry, and Biophysics Institute of Tehran University.

REFERENCES

1. I. Vlasova and A. Saletskii, *Russ. J. Phys. Chem. B*, **3**, No. 6, 976–80 (2009).
2. Z. Tong, J. E. Schiel, E. Papastavros, C. M. Ohnmacht, Q. R. Smith, and D. S. Hage, *J. Chromatogr. A*, **1218**, No. 15, 2065–2071 (2011).
3. J. Kang, Y. Liu, M.-X. Xie, S. Li, M. Jiang, and Y.-D. Wang, *Biochim. Biophys. Acta*, **1674**, No. 2, 205–214 (2004).
4. T. Hanai, A. Koseki, R. Yoshikawa, M. Ueno, T. Kinoshita, and H. Homma, *Anal. Chim. Acta*, **454**, No. 1, 101–108 (2002).
5. V. Lhiaubet-Vallet, Z. Sarabia, F. Boscá, and M. A. Miranda, *J. Am. Chem. Soc.*, **126**, No. 31, 9538–9539 (2004).
6. M. C. Jiménez, M. A. Miranda, and I. Vayá, *J. Am. Chem. Soc.*, **127**, No. 29, 10134–10135 (2005).
7. A. Ahmed-Ouameur, S. Diamantoglou, M. Sedaghat-Herati, S. Nafisi, R. Carpentier, and H. Tajmir-Riahi, *Cell Biochem. Biophys.*, **45**, No. 2, 203–213 (2006).
8. M. Fasano, S. Curry, E. Terreno, M. Galliano, G. Fanali, P. Narciso, et al., *IUBMB Life*, **57**, No. 12, 787–796 (2005).
9. U. Anand and S. Mukherjee, *Biochim. Biophys. Acta*, **1830**, No. 12, 5394–5404 (2013).
10. A. Varshney, P. Sen, E. Ahmad, M. Rehan, N. Subbarao, and R. H. Khan, *Chirality: The Pharmacological, Biological, and Chemical Consequences of Molecular Asymmetry*, **22**, No. 1, 77–87 (2010).
11. G. Calviello, S. Serini, *Dietary Omega-3 Polyunsaturated Fatty Acids and Cancer*, Springer (2010).
12. M. Campagnoli, U. Kragh-Hansen, A. O. Pedersen, A. Amoresano, A. W. Lyon, R. Cesati, et al., *Clin. Biochem.*, **36**, No. 8, 597–605 (2003).
13. P. M. Kris-Etherton, W. S. Harris, and L. J. Appel, *Arteriosclerosis, Thrombosis, and Vascular Biology*, **23**, No. 2, e20–e30 (2003).
14. A. M. Patwardhan, P. E. Scotland, A. N. Akopian, and K. M. Hargreaves, *Proc. Natl. Acad. Sci.*, **106**, No. 44, 18820–18824 (2009).
15. N. Gheibi, M. Ghorbani, H. Shariatifar, and A. Farasat, *PloS One*, **14**, No. 10, e0224095 (see [16]) (2019).
16. N. Gheibi, M. Ghorbani, H. Shariatifar, and A. Farasat, *PloS One*, **15**, No. 3, e0230780 (2020).
17. A. Akya, A. Farasat, K. Ghadiri, and M. Rostamian, *Genetics and Evolution*, **75**, 103953 (2019).
18. N. Gheibi, A. Saboury, K. Haghbeen, F. Rajaei, and A. Pahlevan, *J. Enzyme Inhibition and Med. Chem.*, **24**, No. 5, 1076–1081 (2009).
19. X. Zhang, H. Zhai, R. Gao, J. Zhang, Y. Zhang, and X. Zheng, *Spectrochim. Acta A: Mol. Biomol. Spectrosc.*, **121**, 724–731 (2014).
20. S. Li, K. Huang, M. Zhong, J. Guo, W.-Z. Wang, and R. Zhu, *Spectrochim. Acta A: Mol. Biomol. Spectrosc.*, **77**, No. 3, 680–686 (2010).
21. D. Agudelo, P. Bourassa, J. Bruneau, G. Berube, É. Asselin, and H.-A. Tajmir-Riahi, *PloS One*, **7**, No. 8 (2012).
22. X. Zhang, L. Li, Z. Xu, Z. Liang, J. Su, J. Huang, et al., *PLoS One*, **8**, No. 3, e59106 (2013).

23. D. Weber, L. Milkovic, S. J. Bennett, H. R. Griffiths, N. Zarkovic, and T. Grune, *Redox Biol.*, **1**, No. 1, 226–233 (2013).
24. M. Nigen, V. Le Tilly, T. Croguennec, D. Drouin-Kucma, and S. Bouhallab, *Biochim. Biophys. Acta*, **1794**, No. 4, 709–715 (2009).
25. C. Nick Pace, S. Trevino, E. Prabhakaran, and J. Martin Scholtz, *Philos. Transt. Roy. Soc. London B: Biol. Sci.*, **359**, No. 1448, 1225–1235 (2004).
26. E. Lindahl, B. Hess, and D. Van Der Spoel, *Mol. Model. Ann.*, **7**, No. 8, 306–317 (2001).
27. A. W. Schüttelkopf, D. M. Van Aalten, *Acta Crystallogr. Sec. D: Biol. Crystallogr.*, **60**, No. 8, 1355–1363 (2004).
28. W. F. van Gunsteren, X. Daura, and A. E. Mark, *Encyclopedia of Computational Chemistry*, **2**, Helva Chimica Acta (2002).
29. A. Farasat, F. Rahbarizadeh, G. Hosseinzadeh, S. Sajjadi, M. Kamali, and A. H. Keihan, *J. Biomol. Struct. Dynam.*, **35**, No. 8, 1710–1728 (2017).
30. S. Ashoka, J. Seetharamappa, P. Kandagal, and S. Shaikh, *J. Lumin.*, **121**, No. 1, 179–86 (2006).
31. I. Vekshin, *Biofizika*, **41**, No. 6, 1176–1179 (1996).
32. M. Gokara, V. V. Narayana, V. Sadarangani, S. R. Chowdhury, S. Varkala, D. B. Ramachary, et al., *J. Biomol. Struct. Dynam.*, **35**, No. 10, 2280–2292 (2017).
33. R. M. Abreu, H. J. Froufe, M. J. R. Queiroz, and I. C. Ferreira, *Chem. Biol. Drug Des.*, **79**, No. 4, 530–534 (2012).
34. V. Mohan, A. C. Gibbs, M. D. Cummings, E. P. Jaeger, and R. L. DesJarlais, *Docking: Successes and Challenges. Curr. Pharm. Des.*, **11**, No. 3, 323–333 (2005).
35. Y. Gou, Z. Zhang, D. Li, L. Zhao, M. Cai, Z. Sun, et al., *Drug Deliv.*, **25**, No. 1, 321–329 (2018).
36. N. Shahabadi, S. M. Fili, and S. Kashanian, *J. Coord. Chem.*, **71**, No. 2, 329–341 (2018).
37. N. Shahabadi, B. Bazvandi, and A. Taherpour, *J. Coord. Chem.*, **70**, No. 18, 3186–3198 (2017).
38. C. Chang and M. T. Nickerson, *J. Food Sci. Technol.*, **55**, No. 8, 2850–2861 (2018).